

“Human and Mouse Cross-Reactive” Albumin-Binding Helix–Loop–Helix Peptide Tag for Prolonged Bioactivity of Therapeutic Proteins

Yuto Nakatani, Zhengmao Ye, Yuki Ishizue, Taishi Higashi, Teruko Imai, Ikuo Fujii, and Masataka Michigami*



Cite This: *Mol. Pharmaceutics* 2022, 19, 2279–2286



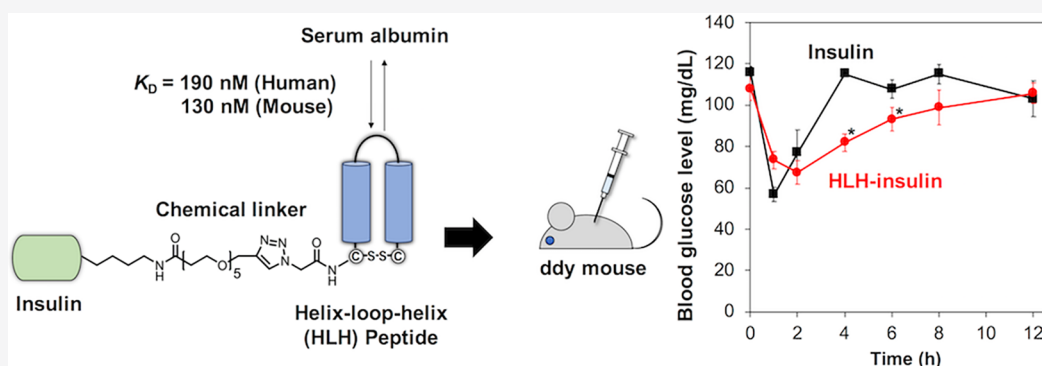
Read Online

ACCESS |

Metrics & More

Article Recommendations

Supporting Information



ABSTRACT: The effectiveness of protein and peptide pharmaceuticals depends essentially on their intrinsic pharmacokinetics. Small-sized pharmaceuticals in particular often suffer from short serum half-lives due to rapid renal clearance. To improve the pharmacokinetics by association with serum albumin (SA) *in vivo*, we generated an SA-binding tag of a helix–loop–helix (HLH) peptide to be linked with protein pharmaceuticals. For use in future preclinical studies, screening of yeast-displayed HLH peptide libraries against human SA (HSA) and mouse SA (MSA) was alternately repeated to give the SA-binding peptide AY-VE, which exhibited cross-binding activities to HSA and MSA with K_D of 65 and 20 nM, respectively. As a proof of concept, we site-specifically conjugated peptide AY-VE with insulin to examine its bioactivity *in vivo*. In mouse bioassay monitoring the blood glucose level, the AY-VE conjugate was found to have a prolonged hypoglycemic effect for 12 h. The HLH peptide tag is a general platform for extending the bioactivity of therapeutic peptides or proteins.

KEYWORDS: CuAAC, helix–loop–helix, insulin, serum albumin, yeast surface display

1. INTRODUCTION

As an alternative to antibodies, downsized affinity molecules with non-immunoglobulin folds are attractive.¹ By using naturally occurring protein scaffolds, a variety of small proteins have been engineered such as designed ankyrin repeat protein,² anticalin,³ monobody,⁴ and truncated Z-domain,⁵ which are used for controlling protein–protein interactions in chemical biology and drug discovery. To advance downsizing, we have developed a conformationally constrained peptide with a *de novo* designed helix–loop–helix (HLH) structure termed a “molecular-targeting HLH peptide” (MW: ~4500).⁶ We have constructed phage- and yeast-displayed libraries of HLH peptides, which have been screened against ganglioside GM1, granulocyte colony stimulating factor receptor (G-CSF-R), cytotoxic T lymphocyte antigen-4 (CTLA-4), and vascular endothelial growth factor to successfully generate molecular-targeting HLH peptides.^{7–10} Due to the rigid constrained conformation, the HLH peptide shows strong binding affinity, high target specificity, and proteolytic

resistance.¹⁰ The small molecular size induces no unwanted immunogenic reactions. In addition, HLH peptides, which consist of natural L-amino acids, are easily produced by conventional chemical synthesis, having the advantages of synthetic simplicity and low-cost manufacture. In this work, an HLH peptide library was used to develop an albumin-binding peptide tag, which was conjugated with a short-lived protein pharmaceutical to improve the pharmacokinetic property.

The effectiveness of recombinant protein pharmaceuticals depends essentially on their intrinsic pharmacokinetics. Small-sized therapeutic proteins and peptides in particular usually suffer from a short serum half-life that leads to low therapeutic

Received: February 10, 2022

Revised: May 19, 2022

Accepted: May 19, 2022

Published: May 28, 2022



efficacy and frequent dosing; this poor bioavailability is commonly due to rapid renal clearance and low stability against proteolytic degradation. Since proteins having a molecular size lower than 70 kDa are efficiently filtered through the glomerular membrane,¹¹ strategies for increasing the molecular size have been developed, such as chemical modification with polyethylene glycol (PEG) and genetic fusion to the Fc fragment of immunoglobulin G or human serum albumin (HSA). In addition, non-covalent association with HSA has been explored as an alternative method.¹² Protein pharmaceuticals have been fused to albumin-binding peptides to increase their half-life *in vivo*.

Here, we describe the generation of a serum albumin (SA)-binding HLH peptide from yeast surface-displayed peptide libraries. From the screening, we isolated HLH peptides with cross-reactivity between HSA and MSA (mouse SA) and explored their biological activity in an animal model. The cross-reactive HLH peptide was site-specifically conjugated to insulin via copper(I)-catalyzed azide–alkyne cycloaddition (CuAAC). Finally, the insulin activity *in vivo* (mouse) was examined by monitoring plasma glucose concentrations, and it showed an extended hypoglycemic effect. HSA-binding HLH peptides can serve as general molecular tags to improve the pharmacokinetics of small-sized therapeutic proteins and peptides.

2. EXPERIMENTAL SECTION

2.1. Yeast Surface Display. The procedures of the library construction were previously described.⁹ In the magnetic-activated cell sorting (MACS) separation, the yeast library was incubated with a mixture of biotinylated HSA and MSA (round 1, 100 nM; round 2, 50 nM; round 3, 25 nM) for 1 h at room temperature. After washing with PBST (PBS with 0.05% Tween 20), the yeast cells were incubated with streptavidin microbeads for 1 h at room temperature and then washed again with PBST. We resuspended the pellet in 7 mL of PBST and applied to the LS column on a magnetic stand. After a wash with PBST, we detached the LS column from the magnetic stand and added 7 mL of SDCAA media into the column to elute the bound yeast cells. The collected cells were grown in SDCAA at 30 °C for 16 h and cultured in SG/RCAA at 20 °C for 24 h to express the HLH peptides on the yeast cell surface.

In the fluorescence-activated cell sorting (FACS) screening, the yeast cells were labeled with mouse anti-FLAG antibody (Sigma-Aldrich), biotinylated HSA, and biotinylated MSA for 1 h. After a wash with PBST, the cells were stained with goat anti-mouse IgG antibody Alexa-488 (Thermo Fisher Scientific) and streptavidin-APC (Thermo Fisher Scientific) for 1 h. The cell sorting was performed on a BD FACS Aria III. The sorted cells were spread onto an SD (–Ura, –Trp) plate.

2.2. Fmoc Solid-Phase Peptide Synthesis. The HLH peptides were synthesized by Fmoc chemistry using an automated peptide synthesizer (PSSM-8, SHIMADZU) on an Fmoc–NH–SAL–PEG resin (substitution: 0.22 mmol/g). After the solid-phase peptide synthesis (SPPS), we performed peptide cleavage with a cocktail containing 2,2,2-trifluoroacetic acid (TFA)/H₂O/triisopropyl silane/1,2-ethanedithiol (94/2.5/2.5/1) at room temperature for 3 h. The peptides were extracted three times using ice-cold diethyl ether. The crude peptides were purified by reverse-phase high-performance liquid chromatography (RP-HPLC) on a C18 column. The fractions were analyzed using matrix-assisted laser desorption

ionization time-of-flight mass spectrometry (MALDI-TOF-MS) (AutoflexII, Bruker Daltonics). The purified peptides (5 mg) were dissolved in 50 mL of 20 mM NH₄HCO₃ (pH 8) and stirred for 12 h to proceed with intramolecular disulfide bond formation. After the reaction, we lyophilized the solution and purified the cyclic peptides by RP-HPLC. All peptides were obtained with a purity >95%.

The N-terminal azidation was performed by the following procedures. Sodium azide (49 mg, 0.75 mmol, 30 equiv) and bromoacetic acid (104 mg, 0.75 mmol, 30 equiv) were reacted in 5 mL of dimethylformamide for 15 h in the dark. The reactant was mixed with *N,N'*-diisopropylcarbodiimide (58 μL, 0.37 mmol, 15 equiv). After 20 min, the solution was reacted with the peptide N-terminus on the resin and stirred for 4 h.

2.3. Surface Plasmon Resonance. Binding affinities were determined using a Biacore T200 instrument (Cytiva). Fatty acid-free HSA (Sigma-Aldrich), fatty acid-free MSA (Sigma-Aldrich), and recombinant human insulin receptor (R&D Systems) were immobilized on a CM5 sensor chip by the standard amine coupling method, and binding responses of the HLH peptides at different concentrations were analyzed in PBST at 25 °C. The data were fitted with a 1:1 kinetic binding model using the Biacore T200 Evaluation Software.

2.4. Circular Dichroism Spectra. Circular dichroism (CD) spectra were acquired using a J-820 spectropolarimeter (Jasco). We collected CD spectra of HLH peptides dissolved in 10 mM phosphate buffer (pH 7.0) at a concentration of 20 μM. The scan speed, response time, and bandwidth were 50 nm/min, 2 s, and 1 nm, respectively.

2.5. Tryptic Digestion Assay. Peptides at concentrations of 150 μM were incubated with trypsin in a substrate/enzyme ratio of 5000:1 at 37 °C in 100 mM Tris–HCl pH 8.0. Aliquots of 10 μL were sampled at different time intervals and mixed with 30 μL of 1 M HCl to stop the reaction. The remaining peptide was detected by RP-HPLC.

2.6. Synthesis of Insulin-Alkyne. Alkyne-PEG5-acid (0.7 mg, 2 μmol), *N*-hydroxysuccinimide (0.3 mg, 2 μmol), and *N,N'*-diisopropylcarbodiimide (0.3 μL, 2 μmol) were dissolved in 100 μL of acetonitrile and stirred for 3 h. Recombinant human insulin (10 mg, 1.8 μmol) was dissolved in 0.3 M Na₂CO₃ (100 μL) and mixed with the active ester for 1 h at room temperature. The reaction was quenched by the addition of 200 mM methylamine (100 μL) and neutralized by 1 M HCl. The product was isolated by RP-HPLC and lyophilized (2.7 mg, 26% yield). HPLC, eluent A: 0.1% TFA in water; eluent B: 0.1% TFA in acetonitrile; linear gradient B: 30–40% over 30 min; column: C-18 (SP-120-5-ODS-RPS, DAISO-PAK).

Site-specific modification was confirmed by the following procedure.¹³ Insulin-alkyne (5 mg) was dissolved in 300 μL of 5 mM dithiothreitol (DTT) in 50 mM Tris–HCl buffer (pH 8.0) and incubated for 30 min at 50 °C. The solution was mixed with 1 mg/mL of trypsin solution (20 μL) for 18 h at 37 °C. To stop the enzymatic reaction, 10% TFA (3 μL) was added. The reactant solution was analyzed by MALDI-TOF-MS.

2.7. Synthesis of AY-VE-Insulin. AY-VE-azide (0.7 mg, 0.2 μmol) and insulin-alkyne (1 mg, 0.2 μmol) were dissolved in 200 μL of water and mixed with 60 mM CuSO₄ (25 μL) and 120 mM sodium *L*-ascorbate (25 μL) for 1 h. The final product was isolated by RP-HPLC (0.7 mg, 40% yield). HPLC, eluent A: 0.1% TFA in water; eluent B: 0.1% TFA in acetonitrile;

linear gradient B: 30–45% over 30 min; column: C-18 (SP-120-5-ODS-RPS, DAISOPAK).

2.8. Hypoglycemic Effect of the AY-VE-Insulin Conjugate. To obtain sample solutions, human insulin, AY-VE-insulin, and YT1-S-insulin (2.3 mg insulin) were dispersed in 100 mL of PBS (pH 7.4) and dissolved by adding 1 N or 10 N HCl solution. After adjusting the pH to 7.4 with 1 N or 10 N NaOH solution, the samples were subcutaneously administrated (38 $\mu\text{g}/\text{kg}$ insulin) to 16 h-fasted healthy ddy mice (6 weeks old, male) (Japan SLC, Inc). At appropriate intervals (0, 1, 2, 4, 6, 8, and 12 h), blood was collected from the jugular veins of the mice anesthetized with isoflurane. The blood glucose concentration was determined using the Glucose-CII-Test Wako (Wako Pure Chemical Industries).

3. RESULTS

3.1. Screening of a Yeast Surface-Displayed HLH Peptide Library for HSA and MSA. A yeast surface-displayed HLH peptide library was constructed based on the HLH peptide scaffold YT1-S. In the scaffold YT1-S (Figure 1A), eight leucine residues inside the two helices make a hydrophobic interaction, which is a driving force to fold the peptide into the HLH structure, and the intramolecular disulfide bond between the N- and C-termini plays an accessory role in the structure stabilization. However, the solvent-exposed residues have no contribution to peptide folding. Therefore, random mutations are introduced into the solvent-exposed positions in YT1-S to give a library of peptides with the HLH structure. We constructed an HLH peptide library by introducing nine random mutations into the loop region (Figure 1A). The degenerate codon NNK (where N = A/C/G/T and K = G/T) covers all 20 amino acids and was used for the randomization. The size of the yeast surface-displayed HLH peptide library was estimated to be 3.0×10^8 by the number of transformants.

The HLH library was screened against HSA and MSA proteins to identify peptides with cross-reactivity: two steps of MACS followed by two steps of FACS. In the first MACS step, the peptide-displayed yeast library was reacted with a mixture of biotinylated HSA and MSA and then captured by using streptavidin-linked magnetic beads. In the second step, the enriched library was screened again for the HSA/MSA mixture and then captured by using anti-biotin antibody-linked magnetic beads to eliminate the streptavidin binders. Since the MACS steps enriched all of the HSA-specific, MSA-specific, and HSA/MSA cross-reactive peptides, we performed further FACS screening to identify the cross-reactive HLH peptides (Figure 1B). The MACS-enriched yeast library was reacted with biotinylated HSA and labeled by streptavidin-APC. The yeast cells with a high fluorescence intensity of APC were sorted by FACS (Figure 2A). After the cell amplification, the yeast library was reacted with biotinylated MSA and then sorted by FACS as well (Figure 2B). The sorted clones were randomly picked up for DNA sequencing to identify the clone AY-01. The HLH peptide AY-01 was then synthesized by Fmoc SPPS (Table S1). After cleavage from the resin, the peptide was cyclized by a disulfide bond between the N- and C-terminal cysteines. The binding affinity of the synthetic peptide AY-01 was examined by surface plasmon resonance (SPR), showing K_D values of 590 ± 90 and 560 ± 160 nM for HSA and MSA, respectively (Figure 2C).

3.2. Affinity Maturation of Cross-Reactive HLH Peptide AY-01. *In vitro* affinity maturation of AY-01 was

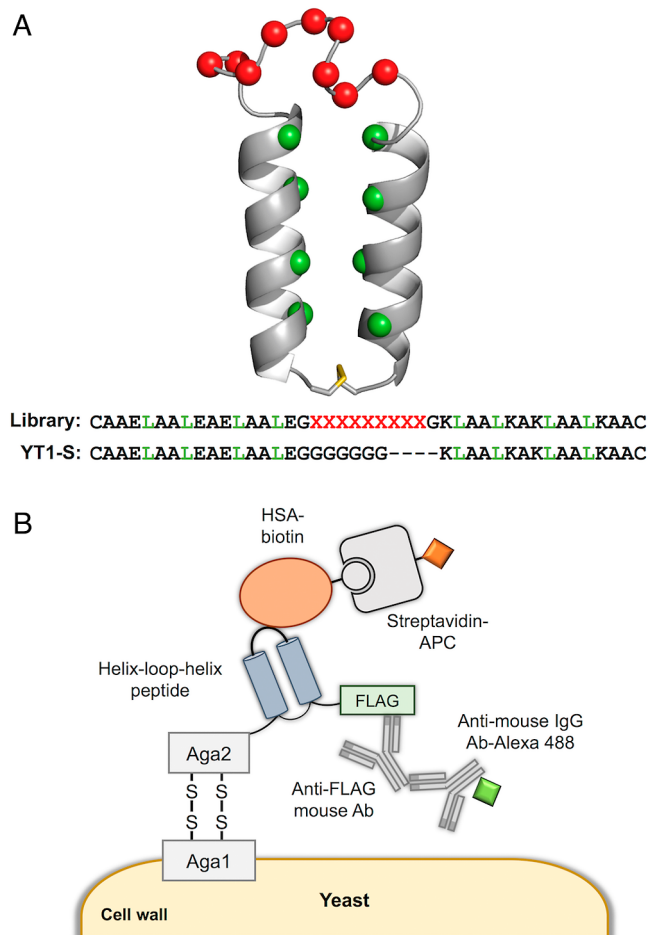


Figure 1. Yeast surface-displayed HLH peptide library. (A) Structural model of the HLH peptide library and the amino acid sequence. Each variable residue (X, red spheres) in the libraries used an NNK degenerate codon that encodes all 20 amino acids. Leu residues located in the hydrophobic core are represented by green spheres. (B) HLH peptide library is displayed on the yeast surface as a fusion with Aga2 protein. The binding to biotinylated SA was detected by using streptavidin-APC. The expression of the HLH peptide library on the cell surface was detected using mouse anti-FLAG antibody and goat anti-mouse IgG antibody-Alexa 488.

conducted to improve its binding activity. A yeast surface-displayed library of AY-01 mutants was constructed by error-prone PCR, which introduced two amino acid mutations per clone on average. The yeast library was screened against biotinylated HSA with a lower concentration (50 nM) by MACS followed by FACS screening (Figure 3A) to give 24 binding peptides. The majority of peptides contained the K28E mutation, and in addition, the peptide loop region possessed the mutation E23V with high frequency (Figure 3B), suggesting that these two mutations were beneficial for HSA binding. The double mutant with E23V/K28E, AY-VE, was synthesized by Fmoc SPPS to evaluate its binding affinity. The HLH peptide AY-VE exhibited improved binding affinities to HSA and MSA with K_D values of 65 ± 39 and 20 ± 3 nM, respectively (Figure 3C). In addition, using FACS to evaluate the cross-reactivity of AY-VE, the yeast clone of AY-VE was reacted with the SAs of multiple species and showed affinity for the albumins of human and mouse, but no affinity to the albumins of cynomolgus monkey and rat (Figure 3D).

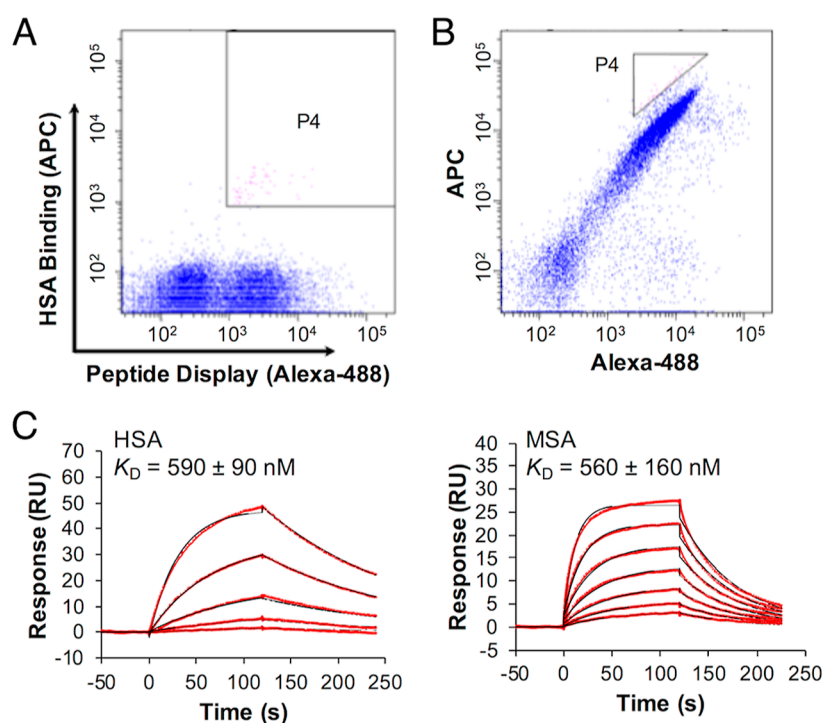


Figure 2. Screening of the yeast surface-displayed HLH peptide library. (A) Dot plots of the initial FACS screening in the presence of 100 nM biotinylated HSA. The yeast cells in the P4 gate were sorted. (B) Dot plots of the second FACS screening in the presence of 100 nM biotinylated MSA. The yeast cells within the P4 gate were collected. (C) Sensorgrams from SPR measurements for binding affinity of the peptide AY-01 to HSA and MSA. AY-01 was injected at concentrations of 125–2000 and 31–2000 nM over immobilized HSA and MSA, respectively. The data were fitted with a 1:1 Langmuir model. Red and black lines indicate the observed sensorgrams and fitting curves, respectively.

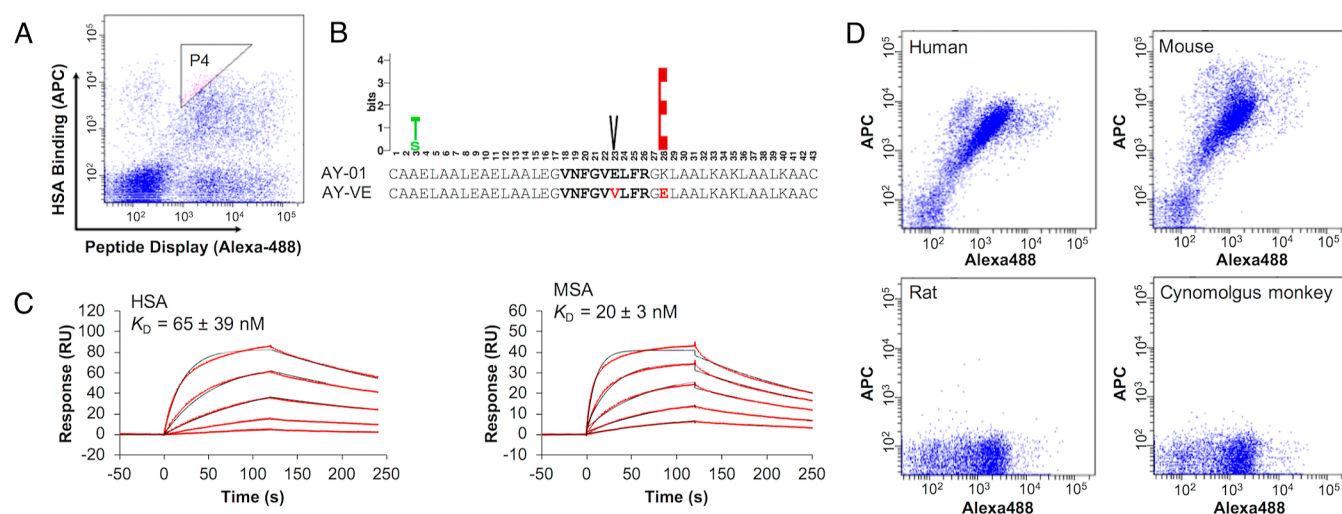


Figure 3. Screening of the yeast surface-displayed library of AY-01 mutants. (A) Dot plots of the final FACS screening of a yeast library of AY-01 mutants in the presence of 50 nM of biotinylated HSA. The yeast cells in the P4 gate were sorted. (B) Sequence logo visualization¹⁴ of the sorted AY-01 mutants and the amino acid sequence of SA-binding peptide. Selected residues from the first library are shown in bold, and mutations after the affinity maturation are shown in red. (C) Sensorgrams of AY-VE for HSA (6–500 nM) and MSA (4–330 nM). Red and black lines indicate the observed sensorgrams and fitting curves, respectively. (D) Binding specificity of AY-VE against SAs from multiple species. The peptide-displayed yeast cells were labeled with mouse anti-FLAG antibody and anti-mouse IgG antibody-Alexa488 conjugate to detect the peptide expression on the cell surface. Binding to biotinylated SAs was labeled with streptavidin-APC. The fluorescence intensities were analyzed by using a flow cytometer.

3.3. Peptide Structural Stability. CD spectra were examined to assess the structural stability of the HLH peptide. As shown in Figure 4A, the peptide AY-VE folded into an α -helical structure that exhibited a positive band at 191 nm and two negative bands at 208 and 222 nm. The structural stability was reversible under heating between 20 and 80 °C; the

spectral magnitude was slightly increased at 80 °C, and then, it returned to the original state with cooling to 20 °C. However, the non-cyclized derivative, AY-VE-dS (Table S2), showed an α -helical structure at 20 °C but not at 80 °C and presented irreversible thermal denaturation (Figure 4B). The C-terminal half-peptide AY-VE-dN, in which the N-terminal helix was

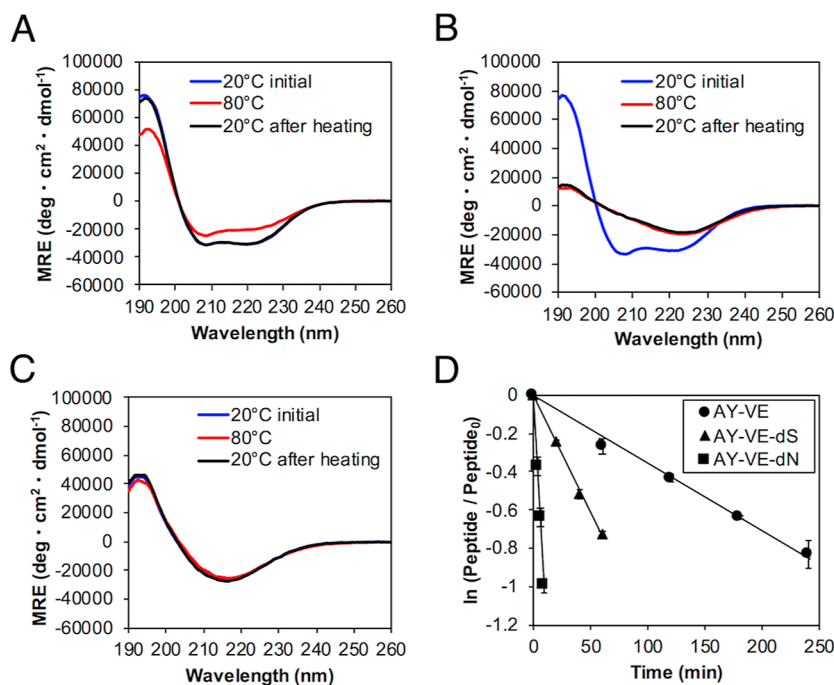


Figure 4. Structural stability of AY-VE and its variants. CD spectra of AY-VE (A), AY-VE-dS (B), and AY-VE-dN (C) at an initial temperature of 20 °C, after incubation at 80 °C for 5 min, and then after cooling down to 20 °C. MRE = mean residue ellipticity. (D) Peptide stabilities against trypsin. The peptides and trypsin were incubated in 0.1 M Tris–HCl at pH 8.0. Natural logarithmic plots of the remaining peptide are represented ($n = 3$).

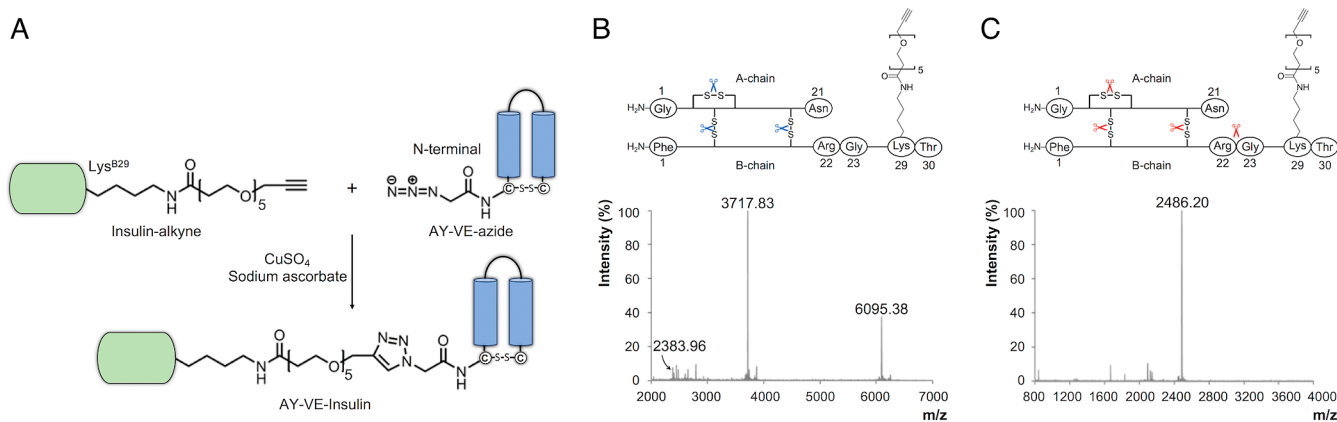


Figure 5. Conjugation of AY-VE and insulin. (A) Synthetic scheme of AY-VE-insulin conjugate. Insulin LysB29 was acylated to give insulin-alkyne. The AY-VE-azide derivative was synthesized by Fmoc SPPS and azidated at the N-terminal amine. These derivatives were conjugated by CuAAC. (B) MALDI-TOF-MS spectrum of the insulin-alkyne using a DAN reductive matrix. A-chain, calculated mass (average isotopes) 2384.74, observed mass 2383.96 (m/z); acylated B-chain, calculated mass (average isotopes) 3717.26, observed mass 3717.83 (m/z); insulin-alkyne, calculated mass (average isotopes) 6094.91, observed mass 6095.38 (m/z) (C) MALDI-TOF-MS spectrum of the insulin-alkyne treated with DTT and trypsin. Insulin B1-22, calculated mass (average isotopes) 2487.2, observed mass 2486.2 (m/z).

deleted, gave an unfolded structure (Figure 4C). The order of stability was AY-VE > AY-VE-dS > AY-VE-dN.

Furthermore, a tryptic digestion assay of the peptides was performed because proteolytic degradation is a major pathway for peptide inactivation *in vivo*. The half-lives of AY-VE, AY-VE-dS, and AY-VE-dN were 190 ± 10 , 56 ± 1 , and 6.3 ± 0.4 min, respectively (Figure 4D). A correlation between peptide structural stability and proteolytic resistance was observed, indicating that a peptide with a highly stable structure was resistant to tryptic digestion.

3.4. Synthesis of the Conjugate of AY-VE and Insulin.

To examine whether the albumin-binding HLH peptide, AY-VE, prolongs the bioactivity of therapeutic proteins *in vivo*, we

synthesized a conjugate of peptide AY-VE and insulin, as shown in Figure 5A. After cleavage of AY-VE azidated at its N-terminal amine on the resin, the AY-VE-azide derivative was cyclized by a disulfide bond in 20 mM ammonium bicarbonate (pH 8). Recombinant human insulin was site-specifically acylated at the ϵ -amino group of LysB29 with an alkyne-PEG5-acid under alkaline conditions (pH > 10).¹⁵ Insulin contains three primary amine groups, the side chain of LysB29 and the N-termini of the two main chains. Therefore, the site-specific acylation was confirmed by MALDI-TOF-MS experiments using 1,5-diaminonaphthalene (DAN) as a reductive matrix.¹⁶ The MS spectrum showed three peaks corresponding to the whole insulin (right, m/z 6095.38), modified B-chain (center,

m/z 3717.83), and A-chain (left, m/z 2383.96) (Figure 5B). In addition, after the insulin-alkyne was treated with DTT and trypsin,¹³ MS showed the highest peak for the B1-22 fragment (m/z 2486.20), indicating no modification of the N-terminal amino group of the B-chain (Figure 5C). Chemical modifications at LysB29 generally do not affect the biological activity.¹⁷ As expected, the SPR analysis showed that the binding affinity of insulin-alkyne ($K_D = 334 \pm 47$ nM) for the insulin receptor was comparable to that of native insulin ($K_D = 380 \pm 75$ nM) (Figure S1).

Finally, the cyclized AY-VE-azide and insulin-alkyne derivatives were linked by CuAAC to give the conjugate AY-VE-insulin. The scaffold YT1-S was also conjugated with insulin in the same manner to give a blank (Figure S2). SPR measurements showed that the conjugate AY-VE-insulin bound to MSA, HSA, and human insulin receptor with K_D values of 130 ± 2 , 190 ± 35 , and 340 ± 14 nM, respectively. The blank conjugate, YT1-S-insulin conjugate, showed no binding to MSA and had binding activity to insulin receptor with a K_D value of 620 ± 12 nM (Table 1, Figure S3). The conjugation thus maintained binding affinity to MSA, HSA, and insulin receptor.

Table 1. Binding Affinities for HSA, MSA, and Insulin Receptor^a

peptide	K_D (nM)		
	HSA	MSA	insulin receptor
AY-01	590 ± 90	560 ± 160	N.T. ^b
AY-VE	65 ± 39	20 ± 3	N.T.
AY-VE-azide	N.T.	38 ± 1	N.D. ^c
AY-VE-insulin	190 ± 35	130 ± 2	340 ± 14
YT1-S-insulin	N.D.	N.D.	620 ± 12
insulin	N.D.	N.D.	380 ± 75

^aData represent mean \pm standard deviation of three independent experiments. ^bN.T.: not tested. ^cN.D.: not determined. The peptide was tested but no measurable value was observed.

3.5. *In Vivo* Bioactivity of the AY-VE-Insulin Conjugate. To evaluate the *in vivo* bioactivity of AY-VE-insulin, blood glucose levels were monitored after subcutaneous administration to healthy mice (Figure 6). Human insulin showed a peak of hypoglycemic effect at 1 h after

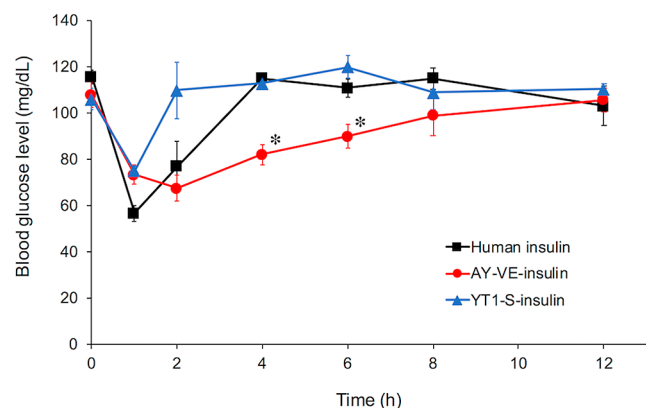


Figure 6. Blood glucose levels after subcutaneous administration of human insulin, AY-VE-insulin, and YT1-S-insulin (38 μ g/kg insulin) to healthy mice. Each point represents the mean \pm S.E of 4–7 experiments. * $p < 0.05$ versus human insulin.

administration. The hypoglycemic effect of YT1-S-insulin was not prolonged and was slightly reduced compared to human insulin. Importantly, AY-VE-insulin exhibited a prolonged hypoglycemic effect for 12 h without a clear peak, suggesting the utility of AY-VE conjugation for extending the bioactivity of therapeutic peptides or proteins.

4. DISCUSSION

In the present study, we generated an HLH peptide that bound to both HSA and MSA to evaluate its efficacy in animal models. In general, the inherent high specificity of antibodies for their target proteins shows limited species cross-reactivity. Therefore, pharmacological evaluation in animal models is performed using surrogate antibodies instead of the candidate antibodies when safety and efficacy are evaluated in preclinical animal models prior to human use. This causes serious problems for the development of therapeutic antibodies, since it is uncertain whether the pharmacological profile exhibited by surrogate antibodies is exactly the same as that of candidate antibodies. As with antibodies, the molecular-targeting HLH peptides show high specificity for their target proteins and limited species cross-reactivity. For use in preclinical studies, we devised a screening method to isolate HLH peptides that bound to both HSA and MSA.

Corresponding to the strong binding of the HLH peptide, AY-VE, to MSA, the *in vivo* bioactivity of AY-VE-insulin was markedly prolonged compared to that of human insulin or YT1-S-insulin (Figure 6). The ability to bind to albumin allows for sustained absorption in subcutaneous tissues and/or long blood retention. So far, insulin therapeutics have been modified with fatty acids to bind to albumin, exhibiting prolonged half-lives. A long-acting insulin detemir possesses myristic acid attached to the side-chain of LysB29.¹⁸ Conjugation of hexadecanoic diacid to insulin at the same position yielded insulin degludec to show a 2.4-fold higher affinity for albumin and a further prolonged half-life.^{19,20} Generally, lipid conjugation is practical for their prolonged blood retention. However, lipidation increases the overall hydrophobicity of the modified biopharmaceuticals that often causes solubility problems. As alternative methods to lipidation, a variety of albumin-binding tags have been reported, for example, albumin-binding small compounds,^{21–28} peptides,^{12,29} antibody fragments,^{30–32} and engineered proteins.^{33–35} Particularly, the peptide tags have advantages in versatility because they can be recombinantly or chemically produced to attach to any protein or peptide therapeutics. A drawback of peptide tags is susceptibility to proteolysis *in vivo*, leading to short half-lives. On the other hand, the HLH peptide, AY-VE, overcomes the drawback by folding into the rigid conformation, which provides high proteolytic resistance. As described in the introduction section, a variety of molecular-targeting HLH peptides have been generated from phage- and yeast-displayed libraries.^{7–10} We expect that grafting of the HSA-binding loop region of AY-VE onto the molecular-targeting HLH peptides would give mid-sized peptide therapeutics with the prolonged bioactivity.

It is noteworthy that the magnitude of the hypoglycemic effect of AY-VE-insulin was retained compared to that of human insulin (Figure 6), even though AY-VE was chemically modified. In general, the PEGylation of insulin causes significant activity loss. For instance, insulin lispro (MW of PEG, 20,000) decreases its activity by 94%.³⁶ PEGylation forms a hydrate layer on the surface of a protein, resulting in a

decrease of affinity to the target molecule. In contrast, the molecular weight of AY-VE is *ca.* 4500, and it has a compact conformation. Thus, the binding affinity of AY-VE-insulin to the insulin receptor was retained, although the activity of YT1-S-insulin was slightly decreased. The conjugation of the HLH peptide AY-VE had a negligible influence on the interaction between the native insulin and insulin receptor. The prolonged absorption and/or blood retention of the AY-VE-insulin conjugate by albumin binding probably resulted in its high hypoglycemic effect.

5. CONCLUSIONS

In this work, molecular-targeting HLH peptides with cross-reactivity to both HSA and MSA were generated from a yeast surface-displayed library. The HLH peptide AY-VE was site-specifically conjugated with insulin as an affinity tag to SA, resulting in prolonged bioactivity of insulin. The high efficacy *in vivo* was due to the highly stable α -helical structure that provides proteolytic stability in plasma. In general, peptides are susceptible to proteolysis by proteases or peptidases due to the amide bonds in their structures. Many approaches are available to enhance the stability of peptides through structural modification, such as replacing L-amino acids with D-amino acids or modification of amino acids (non-natural amino acids and protecting N- and C-termini).³⁷ In contrast, the HLH peptide, which consists of only natural amino acids, gains proteolytic stability through its stable HLH structure. This constrained conformation limits the adoption of binding conformations to the active sites of proteases. The composition of natural amino acids has the advantage of genetic production of HLH-fused recombinant protein pharmaceuticals. Therefore, an HSA-binding HLH peptide tag can serve as a general platform for the engineering of long-acting protein and peptide pharmaceuticals.

■ ASSOCIATED CONTENT

SI Supporting Information

The Supporting Information is available free of charge at <https://pubs.acs.org/doi/10.1021/acs.molpharmaceut.2c00106>.

HPLC, MALDI-TOF-MS analysis, and SPR sensorgrams of the synthetic peptides (PDF)

■ AUTHOR INFORMATION

Corresponding Author

Masataka Michigami – Department of Biological Science, Graduate School of Science, Osaka Prefecture University, Sakai, Osaka 599-8531, Japan; orcid.org/0000-0001-7075-8958; Email: michigami@b.s.osakafu-u.ac.jp

Authors

Yuto Nakatani – Department of Biological Science, Graduate School of Science, Osaka Prefecture University, Sakai, Osaka 599-8531, Japan

Zhengmao Ye – Interprotein Corporation, Osaka 531-0072, Japan

Yuki Ishizue – Graduate School of Pharmaceutical Science, Kumamoto University, Kumamoto 862-0973, Japan

Taishi Higashi – Graduate School of Pharmaceutical Science, Kumamoto University, Kumamoto 862-0973, Japan;

orcid.org/0000-0001-8439-5377

Teruko Imai – Graduate School of Pharmaceutical Science, Kumamoto University, Kumamoto 862-0973, Japan; Daiichi University of Pharmacy, Fukuoka 815-8511, Japan

Ikuo Fujii – Department of Biological Science, Graduate School of Science, Osaka Prefecture University, Sakai, Osaka 599-8531, Japan; orcid.org/0000-0003-2571-546X

Complete contact information is available at:

<https://pubs.acs.org/10.1021/acs.molpharmaceut.2c00106>

Notes

The authors declare the following competing financial interest(s): Z.Y. is an employee of Interprotein Corporation.

■ REFERENCES

- (1) Binz, H. K.; Amstutz, P.; Plückthun, A. Engineering Novel Binding Proteins from Nonimmunoglobulin Domains. *Nat. Biotechnol.* **2005**, *23*, 1257–1268.
- (2) Forrer, P.; Stumpp, M. T.; Binz, H. K.; et al. A Novel Strategy to Design Binding Molecules Harnessing the Modular Nature of Repeat Proteins. *FEBS Lett.* **2003**, *539*, 2–6.
- (3) Beste, G.; Schmidt, F. S.; Stibora, T.; et al. Small Antibody-like Proteins with Prescribed Ligand Specificities Derived from the Lipocalin Fold. *Proc. Natl. Acad. Sci. U.S.A.* **1999**, *96*, 1898–1903.
- (4) Koide, A.; Bailey, C. W.; Huang, X.; et al. The Fibronectin Type III Domain as a Scaffold for Novel Binding Proteins. *J. Mol. Biol.* **1998**, *284*, 1141–1151.
- (5) Braisted, A. C.; Wells, J. A. Minimizing a binding domain from protein A. *Proc. Natl. Acad. Sci. U.S.A.* **1996**, *93*, S688–S692.
- (6) Suzuki, N.; Fujii, I. Optimization of the Loop Length for Folding of a Helix-Loop-Helix Peptide. *Tetrahedron Lett.* **1999**, *40*, 6013–6017.
- (7) Matsubara, T.; Iida, M.; Tsumuraya, T.; et al. Selection of a carbohydrate-binding domain with a helix-loop-helix structure. *Biochemistry* **2008**, *47*, 6745–6751.
- (8) El-Haggar, R.; Kamikawa, K.; Machi, K.; et al. Molecular design of small organic molecules based on structural information for a conformationally constrained peptide that binds to G-CSF receptor. *Bioorg. Med. Chem. Lett.* **2010**, *20*, 1169–1172.
- (9) Mudiyansele, T. M. R.; Michigami, M.; Ye, Z.; et al. An Immune-Stimulatory Helix-Loop-Helix Peptide: Selective Inhibition of CTLA-4/B7 Interaction. *ACS Chem. Biol.* **2020**, *15*, 360–368.
- (10) Michigami, M.; Takahashi, K.; Yamashita, H.; et al. A “Ligand-Targeting” Peptide-Drug Conjugate: Targeted Intracellular Drug Delivery by VEGF-Binding Helix-Loop-Helix Peptides via Receptor-Mediated Endocytosis. *PLoS One* **2021**, *16*, No. e0247045.
- (11) Holecck, M. J. Glomerular filtration: an overview. *Nephrol. Nurs. J.* **2003**, *30*, 285.
- (12) Dennis, M. S.; Zhang, M.; Meng, Y. G.; et al. Albumin binding as a general strategy for improving the pharmacokinetics of proteins. *J. Biol. Chem.* **2002**, *277*, 35035–35043.
- (13) Huang, K.; Huang, T. A novel insulin derivative chemically modified with dehydrocholic acid: synthesis, characterization and biological activity. *Biotechnol. Appl. Biochem.* **2005**, *42*, 47–56.
- (14) Crooks, G. E.; Hon, G.; Chandonia, J.-M.; Brenner, S. E. WebLogo: a sequence logo generator. *Genome Res.* **2004**, *14*, 1188–1190.
- (15) Gao, J.; Mrksich, M.; Gomez, F. A.; Whitesides, G. M. Using capillary electrophoresis to follow the acetylation of the amino groups of insulin and to estimate their basicities. *Anal. Chem.* **1995**, *67*, 3093–3100.
- (16) Fukuyama, Y.; Iwamoto, S.; Tanaka, K. Rapid sequencing and disulfide mapping of peptides containing disulfide bonds by using 1,5-diaminonaphthalene as a reductive matrix. *J. Mass Spectrom.* **2006**, *41*, 191–201.
- (17) Lindsay, D. G.; Shall, S. The acetylation of insulin. *Biochem. J.* **1971**, *121*, 737–745.

- (18) Philips, J.-C.; Scheen, A. Insulin detemir in the treatment of type 1 and type 2 diabetes. *Vasc. Health Risk Manag.* **2006**, *2*, 277–283.
- (19) Kurtzhals, P.; Havelund, S.; Jonassen, I.; et al. Albumin binding of insulins acylated with fatty acids: characterization of the ligand-protein interaction and correlation between binding affinity and timing of the insulin effect in vivo. *Biochem. J.* **1995**, *312*, 725–731.
- (20) Jonassen, I.; Havelund, S.; Hoeg-Jensen, T.; Steensgaard, D. B.; et al. Design of the novel protraction mechanism of insulin degludec, an ultra-long-acting basal insulin. *Pharm. Res.* **2012**, *29*, 2104–2114.
- (21) Koehler, M. F. T.; Zobel, K.; Beresini, M. H.; Caris, L. D.; et al. Albumin affinity tags increase peptide half-life in vivo. *Bioorg. Med. Chem. Lett.* **2002**, *12*, 2883–2886.
- (22) Zobel, K.; Koehler, M. F. T.; Beresini, M. H.; Caris, L. D.; et al. Phosphate ester serum albumin affinity tags greatly improve peptide half-life in vivo. *Bioorg. Med. Chem. Lett.* **2003**, *13*, 1513–1515.
- (23) Dumelin, C. E.; Trüssel, S.; Buller, F.; Trachsel, E.; et al. A portable albumin binder from a DNA-encoded chemical library. *Angew. Chem., Int. Ed.* **2008**, *47*, 3196–3201.
- (24) Trüssel, S.; Dumelin, C.; Frey, K.; Villa, A.; et al. New strategy for the extension of the serum half-life of antibody fragments. *Bioconjugate Chem.* **2009**, *20*, 2286–2292.
- (25) Sasson, K.; Marcus, Y.; Lev-Goldman, V.; Rubinraut, S.; et al. Engineering prolonged-acting prodrugs employing an albumin-binding probe that undergoes slow hydrolysis at physiological conditions. *J. Controlled Release* **2010**, *142*, 214–220.
- (26) Han, J.; Sun, L.; Chu, Y.; Li, Z.; et al. Design, synthesis, and biological activity of novel dicoumarol glucagon-like peptide 1 conjugates. *J. Med. Chem.* **2013**, *56*, 9955–9968.
- (27) Chen, H.; Wang, G.; Lang, L.; Jacobson, O.; et al. Chemical Conjugation of Evans Blue Derivative: A Strategy to Develop Long-Acting Therapeutics through Albumin Binding. *Theranostics* **2016**, *6*, 243–253.
- (28) Bech, E. M.; Martos-Maldonado, M. C.; Wismann, P.; Sørensen, K. K.; et al. Peptide Half-Life Extension: Divalent, Small-Molecule Albumin Interactions Direct the Systemic Properties of Glucagon-Like Peptide 1 (GLP-1) Analogues. *J. Med. Chem.* **2017**, *60*, 7434–7446.
- (29) Zorzi, A.; Middendorp, S. J.; Wilbs, J.; Deyle, K.; et al. Acylated heptapeptide binds albumin with high affinity and application as tag furnishes long-acting peptides. *Nat. Commun.* **2017**, *8*, 16092.
- (30) Coppieters, K.; Dreier, T.; Silence, K.; Haard, H. D.; et al. Formatted anti-tumor necrosis factor alpha VHH proteins derived from camelids show superior potency and targeting to inflamed joints in a murine model of collagen-induced arthritis. *Arthritis Rheum.* **2006**, *54*, 1856–1866.
- (31) Müller, M. R.; Saunders, K.; Grace, C.; Jin, M.; et al. Improving the pharmacokinetic properties of biologics by fusion to an anti-HSA shark VNAR domain. *mAbs* **2012**, *4*, 673.
- (32) Adams, R.; Griffin, L.; Compson, J. E.; Jairaj, M.; et al. Extending the half-life of a fab fragment through generation of a humanized anti-human serum albumin Fv domain: An investigation into the correlation between affinity and serum half-life. *mAbs* **2016**, *8*, 1336–1346.
- (33) Jonsson, A.; Dogan, J.; Herne, N.; Abrahmsen, L.; et al. Engineering of a femtomolar affinity binding protein to human serum albumin. *Protein Eng. Des. Sel.* **2008**, *21*, 515–527.
- (34) Steiner, D.; Merz, F. W.; Sonderegger, I.; Gulotti-Georgieva, M.; et al. Half-life extension using serum albumin-binding DARPin® domains. *Protein Eng. Des. Sel.* **2017**, *30*, 583–591.
- (35) Masuda, Y.; Yamaguchi, S.; Suzuki, C.; Aburatani, T.; et al. Generation and Characterization of a Novel Small Biologic Alternative to Proprotein Convertase Subtilisin/Kexin Type 9 (PCSK9) Antibodies, DS-9001a, Albumin Binding Domain-Fused Anticalin Protein. *J. Pharmacol. Exp. Ther.* **2018**, *365*, 368–378.
- (36) Caparrotta, T. M.; Evans, M. PEGylated insulin Lispro, (LY2605541)—a new basal insulin analogue. *Diabetes Obes. Metabol.* **2014**, *16*, 388–395.
- (37) Di, L. Strategic approaches to optimizing peptide ADME properties. *AAPS J.* **2015**, *17*, 134–143.